Optimization of Gaussian Random Fields

Citation: Dow, Eric, and Qiqi Wang. "Optimization of Gaussian Random Fields." SIAM Journal on Scientific Computing 37, no. 4 (January 2015): A1685–A1704. © 2015, Society for Industrial and Applied Mathematics

As Published: http://dx.doi.org/10.1137/140992187

Publisher: Society for Industrial and Applied Mathematics

Persistent URL: http://hdl.handle.net/1721.1/100548

Version: Final published version: final published article, as it appeared in a journal, conference proceedings, or other formally published context

SIAM J. SCI. COMPUT.
Vol. 37, No. 4, pp. A1685–A1704

OPTIMIZATION OF GAUSSIAN RANDOM FIELDS*

ERIC DOW† AND QIQI WANG†

Abstract. Many engineering systems are subject to spatially distributed uncertainty, i.e., uncertainty that can be modeled as a random field. Altering the mean or covariance of this uncertainty will, in general, change the statistical distribution of the system outputs. We present an approach for computing the sensitivity of the statistics of system outputs with respect to the parameters describing the mean and covariance of the distributed uncertainty. This sensitivity information is then incorporated into a gradient-based optimizer to optimize the structure of the distributed uncertainty to achieve desired output statistics. This framework is applied to perform variance optimization for a model problem and to optimize the manufacturing tolerances of a gas turbine compressor blade.

Key words. random fields, pathwise sensitivity method, optimization

AMS subject classifications. 49N45, 60G15, 60G60

DOI. 10.1137/140992187

1. Introduction and motivation.

An engineering system maps a set of inputs to a set of outputs, which quantify the performance of the system. In a deterministic design setting, the inputs are assumed to take a single (nominal) value, and the resulting outputs are deterministic functions of the nominal input values. In many engineering systems, the inputs are subject to some uncertainty due to natural variations in the system's environment or due to a lack of knowledge. In this case, the inputs can be modeled as random variables, and the system outputs are also, in general, random variables. The system performance is commonly quantified in terms of the statistics of the outputs, e.g., their mean or variance. The statistical distribution of the system outputs can be changed by either changing the distribution of the input uncertainty, or by changing the design of the system, i.e., how the inputs are mapped to the outputs. Design under uncertainty, also referred to as robust design, is often applied to optimize systems with random outputs. Broadly speaking, robust design methodologies construct designs whose performance remains relatively unchanged when the inputs are perturbed from their nominal value as a result of uncertainty [3]. Examples include topology optimization of structures subject to random field uncertainties, design of gas turbine compressor blades subject to manufacturing variations, and optimization of airfoils subject to geometric uncertainty [7, 14, 29]. In these works, the system design is optimized to minimize the impact of variability on the output statistics.

In most applications of robust optimization, the statistical distribution of the input variability is assumed to be constant. In some applications, however, the distribution of the input uncertainty can be controlled. A concrete example is a gas turbine compressor blade subject to geometric variability introduced by the manufacturing process. The random error introduced to the blade geometry by the manufacturing process is an example of spatially distributed uncertainty, and can therefore be modeled as a random field. The mean performance of manufactured compressor blades has

*Submitted to the journal's Methods and Algorithms for Scientific Computing section October 20, 2014; accepted for publication (in revised form) May 15, 2015; published electronically July 8, 2015.
http://www.siam.org/journals/sisc/37-4/99218.html
†Department of Aeronautics and Astronautics, Massachusetts Institute of Technology, Cambridge, MA 02139 (ericdow@mit.edu, qiqi@mit.edu).

been shown to degrade as the level of variability (quantified by its standard deviation) increases [14]. The level of variability can be reduced by specifying stricter manufacturing tolerances. However, specifying stricter manufacturing tolerances incurs higher manufacturing costs. Therefore, the cost associated with reducing variability competes with the benefits of improving performance, implying that there may be some optimal level of variability that balances these competing costs. Controlling the level of uncertainty has applications in other fields, such as oil reservoir simulation, where the subsurface properties are unknown and therefore modeled as random fields. Making direct measurements of these properties reduces the level of uncertainty in the model, allowing oil extraction to be performed more efficiently, but incurs additional costs of performing field measurements.

This paper presents a method for optimizing the statistical distribution of random fields that describe the variability in a system's inputs. An efficient approach for computing the sensitivity of system outputs with respect to the parameters defining the distribution of the random field is presented. This sensitivity information is then used by a gradient-based optimizer to optimize these parameters. We apply this framework to perform variance optimization for a model problem as well as to a compressor blade tolerance optimization problem.

2. Gaussian random fields. Random fields provide a convenient method for modeling spatially distributed uncertainty. Random fields have previously been used to model spatially distributed uncertainty in a wide variety of systems, including natural variations in ground permeability [8], random deviations in material properties for structural optimization problems [7], and geometric variability in airfoils [5, 29]. In this work, we consider spatially distributed uncertainty in the form of a Gaussian random field $e(x, \theta)$ where x indexes a metric space X and θ indexes the sample space Θ. The defining characteristic of Gaussian random fields is that for any $x_1, \ldots, x_n$, the vector $(e(x_1, \theta), \ldots, e(x_n, \theta))$ is distributed as a multivariate Gaussian. Gaussian random fields are uniquely defined by their mean $\bar{e}(x)$ and covariance function $C(x_1, x_2)$:

$$\bar{e}(x) = \mathbb{E}[e(x, \theta)], \tag{2.1}$$

$$C(x_1, x_2) = \mathbb{E}[(e(x_1, \theta) - \bar{e}(x_1))(e(x_2, \theta) - \bar{e}(x_2))], \tag{2.2}$$

where the expectation is taken over θ. The covariance function describes the smoothness and correlation length of the random field.

2.1. The Karhunen–Loève expansion. The Karhunen–Loève (K-L) expansion, also referred to as the proper orthogonal decomposition (POD), can be used to represent a random field as a spectral decomposition of its covariance function [22]. The K-L expansion of a random field with mean $\bar{e}(x)$ and covariance function $C(x_1, x_2)$ is given by

$$e(x, \theta) = \bar{e}(x) + \sum_{i \geq 1} \sqrt{\lambda_i} \phi_i(x) \xi_i(\theta), \tag{2.3}$$

where the eigenvalues λ_i and eigenfuctions $\phi_i(x)$ are computed from the following Fredholm equation:

$$\int_S C(x_1, x_2) \phi_i(x_2) dx_2 = \lambda_i \phi_i(x_1). \tag{2.4}$$

The random coefficients $\xi_i(\theta)$ are mutually uncorrelated with zero mean and unit variance. For a Gaussian random field, the $\xi_i(\theta)$ are independently and identically distributed (i.i.d.) standard normal random variables.

To construct the K-L expansion numerically, the Nyström method is used [25]. The domain X is discretized, and Gaussian quadrature is used to approximate the integral in (2.4). This results in a discrete eigenproblem of the form

$$\mathbf{C}\phi_i = \lambda_i \phi_i, \tag{2.5}$$

where $\mathbf{C}$ is the discretized covariance matrix. Solving this eigenproblem gives the eigenvalues and eigenvectors evaluated on the discretized domain. The K-L expansion (2.3) is truncated at a finite number of terms, resulting in an approximate spectral expansion of the random field

$$\hat{e}(x,\theta) = \bar{e}(x) + \sum_{i=1}^{N_{KL}} \sqrt{\lambda_i}\phi_i(x)\xi_i(\theta). \tag{2.6}$$

The truncated expansion minimizes the mean square error, and the decay of the eigenvalues determines the rate of convergence. The level of truncation N_{KL} is often set equal to the smallest k such that the partial scatter S_k exceeds some threshold, where the partial scatter is defined as

$$S_k = \frac{\sum_{i=1}^{k} \lambda_i}{\sum_{i=1}^{N_s} \lambda_i}. \tag{2.7}$$

3. Optimizing the mean and covariance. Consider a system whose performance is subject to spatially distributed uncertainty in the form of a Gaussian random field $e(x,\theta)$. Each output of the system is a functional of this random field, i.e., $F(\theta) = F(e(x,\theta))$, and is itself a random variable. F can either be a direct functional of the random field, or a functional of the solution of a system of equations subject to random field uncertainty. We are interested in the statistics s_F of this functional, e.g., its mean or variance. In the case of multiple system output statistics, we generalize to the vector of output statistics $\mathbf{s_F}$.

We aim to optimize the system's statistical response s_F by controlling the mean and covariance of the random field $e(x,\theta)$. The design variables are then the mean of the random field $\bar{e}(x)$, parameterized by the vector $\mathbf{p}_m$, and covariance of the random field $C(x_1,x_2)$, parameterized by the vector $\mathbf{p}_c$. The design vector $\mathbf{p} = \{\mathbf{p}_m, \mathbf{p}_c\}$ fully defines the Gaussian random field. We assume that $\bar{e}(x;\mathbf{p}_m)$ and $C(x_1,x_2;\mathbf{p}_c)$ depend smoothly on $\mathbf{p}_m$ and $\mathbf{p}_c$, respectively. Changing the mean and covariance of the random field will, in general, change the system output statistics, so that $s_F = s_F(\mathbf{p})$. Figure 1 illustrates the propagation of the random field to the output statistic $s_F = \mathbb{E}[F]$.

To optimize the statistical response of the system, we formulate the following optimization problem:

$$\begin{aligned} \mathbf{p}^* = \quad & \underset{\mathbf{p}\in\mathcal{P}}{\arg\min} \quad f(\mathbf{p}, \mathbf{s_F}(\mathbf{p})) \\ & \text{s.t.} \quad g(\mathbf{p}, \mathbf{s_F}(\mathbf{p})) \le 0, \\ & \qquad\quad h(\mathbf{p}, \mathbf{s_F}(\mathbf{p})) = 0, \end{aligned} \tag{3.1}$$

where the objective and constraint functions f, g, and h may depend on both the design parameters $\mathbf{p}$ and the system output statistics $\mathbf{s_F}(\mathbf{p})$, and $\mathcal{P}$ denotes the design

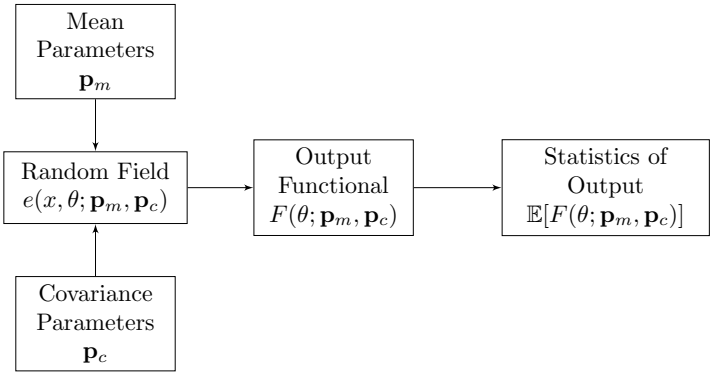

FIG. 1. *Propagation of distributed uncertainty to the statistics of an output quantity of interest (in this case, the mean of the functional F).*

space for the mean and covariance parameters. In general, the objective and constraint functions are nonlinear with respect to $\mathbf{p}$.

4. Sample average approximation. To solve (3.1), we employ a gradient-based approach that incorporates sensitivity information to accelerate convergence to an optimal solution. Specifically, the sample average approximation (SAA) method, also referred to as sample path optimization, is used to optimize the mean and covariance of the random field [28]. We limit our attention to the special case where each objective and constraint functions are equal to the mean of an output functional, since this special case encompasses the problems of interest in this work.

In the SAA method, the objective functions and constraints are approximated using the Monte Carlo method. For example, the mean of the functional $F(e)$ is estimated as

$$\mathbb{E}[F] \approx \frac{1}{N}\sum_{n=1}^{N} F_n. \tag{4.1}$$

The process for propagating distributed uncertainty to the quantities of interest is summarized as follows:

1. Generate a $N \times N_{KL}$ matrix of independent Gaussian random variables.
2. For each Monte Carlo sample, construct a realization of the random field $e_n(x)$ using the K-L expansion (2.6).
3. Evaluate the functional of interest $F_n = F(e_n)$ for each realization.
4. Estimate the moments of F according to (4.1).

The convergence rate of the Monte Carlo estimate (4.1) is $O(N^{-1/2})$, and therefore a large number of Monte Carlo samples are typically required. However, the Monte Carlo samples can be evaluated in parallel, greatly reducing the wall time required to evaluate (4.1).

The SAA method transforms the stochastic optimization problem (3.1) into a deterministic optimization problem. This is achieved by fixing the set of realizations $\{\boldsymbol{\xi}_n\}_{n=1}^N$ of the random input vector used to compute the Monte Carlo estimates of the objective and constraint functions. The SAA method therefore solves the following modified optimization problem, where the objective and constraint functions have

been replaced by their Monte Carlo estimates:

$$\begin{aligned} \hat{\mathbf{p}}_N^* = \quad & \underset{\mathbf{p}\in\mathcal{P}}{\arg\min} \quad \hat{f}_N(\mathbf{p}) \\ & \text{s.t.} \quad \hat{g}_N(\mathbf{p}) \le 0, \\ & \qquad \hat{h}_N(\mathbf{p}) = 0. \end{aligned} \tag{4.2}$$

The subscript N has been added to emphasize the number of samples used to construct the estimators. The deterministic optimization problem that results from fixing the samples can be solved iteratively to update the solution, using the same set of realizations $\{\boldsymbol{\xi}_n\}_{n=1}^N$ at each iteration. The solution of the deterministic optimization problem, denoted $\hat{\mathbf{p}}_N^*$, is an estimator of the true solution $\mathbf{p}^*$.

The reduction of the stochastic optimization problem into a deterministic optimization problem allows for the use of one of many algorithms designed for the efficient solution of deterministic optimization problems. Thus, the SAA method is well suited to solve constrained stochastic optimization problems. A convergence rate of $N^{-1/2}$ for the constrained problem can also be observed under certain conditions [28]. Numerous methods have been devised for solving deterministic optimization problems with both nonlinear objectives and nonlinear constraints. One such method, the sequential quadratic programming (SQP) method, is reviewed next.

4.1. Sequential quadratic programming. An efficient approach to solving (4.2) is the SQP method. Given an approximate solution $\hat{\mathbf{p}}^k$, the SQP solves a quadratic programming subproblem to obtain an improved approximate solution $\hat{\mathbf{p}}^{k+1}$. This process is repeated to construct a sequence of approximations that converge to a solution $\hat{\mathbf{p}}^*$ [4]. The quadratic subproblems are formed by first constructing the Lagrangian function from the objective and constraint functions. A quadratic objective is constructed from the second-order Taylor series expansion of the Lagrangian, and the constraints are replaced with their linearizations. The solution of the quadratic subproblem produces a search direction, and a linesearch can be applied to update the approximate solution. To construct the second-order Taylor series of the Lagrangian, the Hessian is estimated using a quasi-Newton update formula, such as the Broyden–Fletcher–Goldfarb–Shanno (BFGS) formula [24]. Local convergence of the SQP algorithm requires that the initial approximate solution is close to a local optimum and that the approximate Hessian is close to the true Hessian. Global convergence requires sufficient decrease in a merit function that measures the progress towards an optimum. More details on local and global convergence of SQP methods can be found in [4].

5. Sensitivity analysis of Gaussian random fields. In this section, we perform sensitivity analysis of a system's output statistics with respect to the mean and covariance of Gaussian random field input uncertainty. This sensitivity information is used to optimize the mean and covariance functions via the SAA method described in the previous section.

5.1. Pathwise sensitivities. To compute the sensitivity of an output statistic, e.g., $\nabla_p \mathbb{E}[F(p)]$, we use the pathwise sensitivity method. The pathwise sensitivity method relies upon interchanging the differentiation and expectation operators. For example, to compute an unbiased estimator of the gradient of $f = \mathbb{E}[F(\theta, \mathbf{p})]$ with respect to a parameter p, we simply interchange differentiation and integration:

$$\frac{\partial}{\partial p}\mathbb{E}[F(\theta,\mathbf{p})] = \mathbb{E}\left[\frac{\partial}{\partial p}F(\theta,\mathbf{p})\right]. \tag{5.1}$$

Sufficient conditions that allow for this interchange will be discussed subsequently.

The pathwise sensitivity method can be applied directly to the Monte Carlo estimate of $\mathbb{E}[F(\theta, \mathbf{p})]$. Replacing the expectation with its Monte Carlo estimate, and exchanging summation and differentiation, gives

$$\mathbb{E}\left[\frac{\partial F}{\partial p}\right] \approx \frac{\partial \hat{f}_N}{\partial p} = \frac{1}{N}\sum_{n=1}^{N}\frac{\partial F_n}{\partial p}. \tag{5.2}$$

In the context of the SAA method, the derivatives $\partial F_n/\partial p$ represent the sensitivity of the random functional $F(\theta, \mathbf{p})$ for a particular realization of the random field $e_n \equiv e(x, \boldsymbol{\xi}_n)$ where all random inputs are held fixed. To compute the sensitivity $\partial F_n/\partial p$, we first apply the chain rule to rewrite this sensitivity:

$$\frac{\partial F_n}{\partial p} = \frac{\partial F_n}{\partial e_n}\frac{\partial e_n}{\partial p}. \tag{5.3}$$

If the functional F depends explicitly on the random field e, the derivative $\partial F_n/\partial e_n$ can be computed directly. As mentioned previously, F may alternatively be a functional of the solution of some system of equations depending on e. In that case, the derivative $\partial F_n/\partial e_n$ can be computed efficiently using the adjoint method [16].

There are a number of alternative methods for estimating $\mathbb{E}[F(\theta, \mathbf{p})]$. One alternative is to apply quadrature to approximate the multidimensional integral using either a tensor product grid or Smolyak sparse grid constructed from one-dimensional quadrature rules [15]. The stochastic dimension associated with spatially distributed uncertainty is typically too large to be handled using quadrature, whose cost grows exponentially with the stochastic dimension. The computational cost of the Monte Carlo method is independent of the stochastic dimension, which is an attractive feature in the present context. Another alternative are so-called sensitivity based methods, which use the sensitivity of the functional F with respect to the random variables $\boldsymbol{\xi}$ to estimate the mean and variance of F [27]. A Taylor series approximation of F is constructed about the mean vector $\bar{\boldsymbol{\xi}}$, and the mean of F can be estimated by taking the mean of the Taylor series. The advantage of this approach is that if the sensitivities can be estimated accurately, the mean and variance can be estimated very rapidly. However, these approximations may be inaccurate when the Taylor series approximation is not an accurate approximation of the true function F.

5.2. Sample path sensitivities. We consider computing the sensitivity of the sample path $e_n \equiv e(x, \boldsymbol{\xi}_n; \mathbf{p}_m, \mathbf{p}_c)$ with respect to the parameters which control the mean and covariance of the random field, i.e., the $\mathbf{p}_m$ and $\mathbf{p}_c$ introduced previously. The sensitivity of the sample path with respect to any parameter p_m controlling the mean can be analytically derived from the K-L expansion given by (2.6). Since the eigenvalues and eigenvectors in the K-L expansion are independent of p_m, only the first term in the K-L expansion depends on p_m. Thus, we have

$$\frac{\partial e_n}{\partial p_m} = \frac{\partial \bar{e}}{\partial p_m}. \tag{5.4}$$

Computing the sensitivity of the sample path with respect to a parameter p_c controlling the covariance is more involved. The pathwise sensitivity method has typically been applied to problems in computational finance and chemical kinetics where the sample paths of the random process can be differentiated analytically with

respect to the parameters of interest [6, 30]. However, the sample path sensitivity of a random field cannot, in general, be differentiated analytically with respect to a parameter controlling the covariance matrix. For a Gaussian random field, we can use its K-L expansion to compute these sensitivities using eigenvalue/eigenvector perturbation theory. We focus on computing the sensitivities of the discretized random field, since numerical computation of the pathwise sensitivity estimate is the ultimate goal. We first consider the general case of computing the sensitivity of the sample path with respect to a covariance parameter p_c, and then the special case where the parameter of interest controls the variance of a random field with fixed correlation function.

5.2.1. General case. Since the covariance matrix is a function of p_c, its eigenvalues and eigenvectors are also functions of p_c. Applying the chain rule to the K-L expansion, we have

$$\frac{\partial e_n}{\partial p_c} = \sum_{i=1}^{N_{KL}} \left(\frac{1}{2\sqrt{\lambda_i}} \phi_i \frac{\partial \lambda_i}{\partial p_c} + \sqrt{\lambda_i} \frac{\partial \phi_i}{\partial p_c} \right) \xi_i(\theta_n). \tag{5.5}$$

Since the pathwise sensitivity approach is used, the random variables $\xi_i(\theta_n)$ remain fixed. Equation (5.5) is only valid if the eigenvalues and eigenvectors in the K-L expansion are differentiable functions of p_c. It can be shown, via the implicit function theorem, that if the eigenvalues of $\mathbf{C}$ are simple (i.e., have algebraic multiplicity one), then the eigenvalues and eigenvectors of $\mathbf{C}$ are infinitely differentiable with respect to p_c [23]. If the eigenvalues remain simple as p_c is varied over some range of values, then the eigenvalues and eigenvectors are differentiable over that range of p_c.

When the eigenvalues are simple, the derivatives of the eigenvalues and eigenvectors can be computed using established results from eigenvalue perturbation theory:

$$\frac{\partial \lambda_i}{\partial p_c} = \phi_i^{\mathsf{T}} \frac{\partial \mathbf{C}}{\partial p_c} \phi_i \tag{5.6}$$

and

$$\frac{\partial \phi_i}{\partial p_c} = -(\mathbf{C} - \lambda_i \mathbf{I})^{+} \frac{\partial \mathbf{C}}{\partial p_c} \phi_i, \tag{5.7}$$

where $(\mathbf{C} - \lambda_i \mathbf{I})^{+}$ denotes the Moore–Penrose pseudoinverse of the matrix $(\mathbf{C} - \lambda_i \mathbf{I})$ [9]. Since the explicit dependence of the entries of the covariance matrix $\mathbf{C}$ on p_c is assumed to be known, the sensitivities of the eigenvalues and discretized eigenvectors in the K-L expansion can be computed in closed form.

One practical issue that arises when using the pathwise sensitivity method results from the sign ambiguity of the eigenvectors. Specifically, although the eigenvector $\phi_i(p_c)$ is differentiable with respect to p_c (and therefore continuous), perturbing p_c by some small ε may result in $\phi_i(p_c + \varepsilon)$ being very different from $\phi_i(p_c)$ as a result of sign ambiguity. This issue is resolved by choosing the sign that results in the "closer" eigenvector: if $\|\phi_i(p_c+\varepsilon)+\phi_i(p_c)\|_2 < \|\phi_i(p_c+\varepsilon)-\phi_i(p_c)\|_2$, then the sign of $\phi_i(p_c+\varepsilon)$ is flipped.

5.2.2. Special case: Sensitivity with respect to the variance. Computing the sample path sensitivities can be simplified if the parameter p_c only scales the variance of the random field, but does not change its correlation function. Consider a

random field $\tilde{e}(x,\theta)$ with unit variance, i.e., $\mathbb{E}[\tilde{e}^2(x,\theta)] = 1$ everywhere. Scaling this random field by the function $\sigma(x)$ produces the random field $e(x,\theta) = \sigma(x)\tilde{e}(x,\theta)$ with nonstationary variance $\sigma^2(x)$ [1]. The covariance function of the process $\tilde{e}(x,\theta)$, denoted $\rho(x_1,x_2)$, satisfies the property $x_1 = x_2 \implies \rho(x_1,x_2) = 1$. The corresponding covariance function of the scaled process $e(x,\theta)$ is given by $\mathbf{C}(x_1,x_2) = \sigma(x_1)\sigma(x_2)\rho(x_1,x_2)$.

Suppose the function $\sigma(x)$ depends smoothly on the parameters $\mathbf{p}_c$. Rather than simulating the random field $e(x,\theta)$ with nonstationary variance, we instead simulate the unit variance field $\tilde{e}(x,\theta)$ and set $e_n(x) = \sigma(x)\tilde{e}_n(x)$. Then, the sample path sensitivity with respect to p_c can be computed as

$$\frac{\partial e_n}{\partial p_c} = \frac{\partial e_n}{\partial \sigma}\frac{\partial \sigma}{\partial p_c} = \tilde{e}_n \frac{\partial \sigma}{\partial p_c}. \tag{5.8}$$

This greatly simplifies the sensitivity calculation since the K-L expansion need only be computed once. This eliminates the issues caused by the sign ambiguity of the eigenvectors since the same set of eigenvectors are used throughout the optimization. The computational cost of performing optimization with this approach is also lower since it does not require the sensitivity of the K-L expansion to be computed at each optimization step. However, this difference in computational cost may be small compared to the cost of computing the objective and constraint function estimates, which typically require many Monte Carlo simulations to be performed. If each Monte Carlo sample is computationally expensive, e.g., requires solving a system of partial differential equations, then the relative savings will be very small.

Figure 2 illustrates scaling a random field with stationary variance to produce realizations of a random field with a spatially varying variance. The original random field, shown at the top, is a zero-mean Gaussian random field with a squared exponential covariance function. The scaled random field, shown on the bottom, is also a zero-mean Gaussian random field. However, the increase in the standard deviation near $x = 0$ produces realizations with more variability in this region than the original random field with stationary variance.

5.3. Interchanging differentiation and expectation. As mentioned previously, applying the pathwise sensitivity method requires that the interchange of differentiation and integration is justified. We now address which conditions on F and $\mathbf{p}$ ensure that this interchange is justified. The first requirement is that the random vector $\boldsymbol{\xi}$ must be independent of the parameters $\mathbf{p}$. Since we use the K-L expansion to simulate the random field, this is true by construction: changing the parameters $\mathbf{p}$ only changes the eigenvalues and eigenvectors in the K-L expansion, thus the random vector $\boldsymbol{\xi}$ is independent of the parameters $\mathbf{p}$.

The second requirement is on the regularity of the function $F(\theta,p)$ (for simplicity, we only consider a single parameter p). Interchanging differentiation and integration requires that the following interchange of limit and integration is justified:

$$\mathbb{E}\left[\lim_{h\to 0}\frac{F(\theta,p+h)-F(\theta,p)}{h}\right] = \lim_{h\to 0}\mathbb{E}\left[\frac{F(\theta,p+h)-F(\theta,p)}{h}\right]. \tag{5.9}$$

A necessary and sufficient condition for this interchange to be valid is that the difference quotients $Q_h = h^{-1}[F(\theta,p+h) - F(\theta,p)]$ are uniformly integrable, i.e., that

$$\lim_{c\to\infty}\sup_h \mathbb{E}[|Q_h|\mathbf{1}\{|Q_h| > c\}] = 0, \tag{5.10}$$

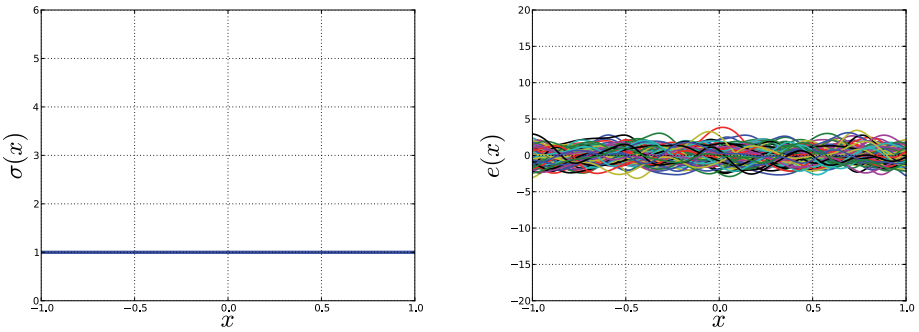

(a) Stationary standard deviation (left) and resulting realizations (right).

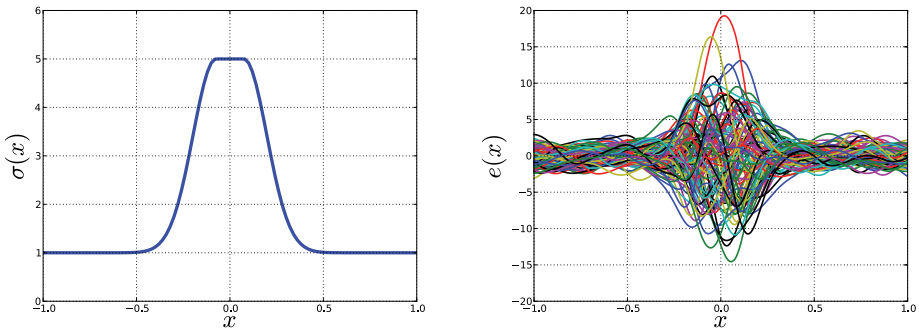

(b) Nonstationary standard deviation (left) and resulting realizations (right).

FIG. 2. *Random fields with stationary (top) and nonstationary (bottom) standard deviation.*

where $\mathbf{1}\{|Q_h| > c\}$ is the indicator function. This condition is not readily verified for practical problems, since the analytical distribution of F is typically unknown. We instead provide a set of sufficient conditions that are more straightforward to verify in practice, following [17]. Recall that F is a functional of the random field $e(\theta, x; p)$, and denote by $D_F \subset \mathbb{R}^{|\Theta|}$ the set of points in Θ where F is differentiable with respect to e. The following are sufficient conditions for the interchange of the limit and expectation in (5.9):

(A1) For every $p \in \mathcal{P}$ and $x \in X$, $\partial e(x, \theta; p)/\partial p$ exists with probability 1.

(A2) For every $p \in \mathcal{P}$, $\mathbb{P}[e(x, \theta; p) \in D_F] = 1$.

(A3) F is Lipschitz continuous, i.e., there exists a constant $k_F < \infty$ such that for all $u(x)$, $v(x)$,

$$|F(u) - F(v)| \leq k_F \|u - v\|. \tag{5.11}$$

(A4) For every $x \in X$, there exists a random variable k_e such that for all p_1, $p_2 \in \mathcal{P}$,

$$|e(x, \theta; p_2) - e(x, \theta; p_1)| \leq k_e |p_2 - p_1|, \tag{5.12}$$

and $\mathbb{E}[k_e] < \infty$.

Conditions (A3) and (A4) imply that F is Lipschitz continuous in p with probability one. Taking $\kappa_F = k_F \sup_x k_e$,

$$|F(\theta, p_2) - F(\theta, p_1)| \leq \kappa_F |p_2 - p_1|. \tag{5.13}$$

We can then bound the difference quotient

$$\left|\frac{F(\theta, p+h) - F(\theta, p)}{h}\right| \leq \kappa_F, \tag{5.14}$$

and apply the dominated convergence theorem to interchange the expectation and limit in (5.9). Thus, conditions (A1)–(A4) are sufficient conditions for the pathwise sensitivity estimate to be unbiased.

Conditions (A3) and (A4) together determine if F is almost surely Lipschitz continuous, and thus determine what type of input parameters and output quantities of interest can be treated with the pathwise sensitivity method. The previous section gave conditions for the differentiability of the sample paths, i.e., that the covariance function depends smoothly on $\mathbf{p}$ and have simple eigenvalues. Output functionals that may change discontinuously when smooth perturbations are made to the random field are not Lipschitz continuous almost surely. Thus, condition (A3) excludes failure probabilities, e.g., $\mathbb{P}(F \geq c) = \mathbb{E}[\mathbf{1}\{F \geq c\}]$, since the indicator function $\mathbf{1}\{F \geq c\}$ is discontinuous when $F = c$. This difficulty can be remedied to some degree using a smoothed version of the indicator function, but this introduces additional error to the sensitivity [12]. Conditions (A2) and (A3) do permit functions that fail to be differentiable at certain points, as long as the points at which differentiability fails occur with probability zero, and F is continuous at these points.

6. Application: Variance optimization. To demonstrate the proposed optimization framework, we consider an optimization problem with the design variables being the variance of a random field. The random field $e(x, \theta)$ is defined on the domain $X = [0, 1]$ and has a squared exponential correlation function:

$$\rho(x_1, x_2) = \exp\left[-\frac{(x_1 - x_2)^2}{2L^2}\right], \tag{6.1}$$

with correlation length $L = 0.1$. The variance $\sigma^2(s)$ of the random field is a spatially dependent function. We seek to minimize the sum of two competing cost functions that depend on $\sigma(s)$ as a (spatially varying) parameter. The first cost function penalizes variability:

$$f_1 = \mathbb{E}\left[\int_0^1 e^2(s, \theta) w(s)\, ds\right], \tag{6.2}$$

where $w(s)$ is a nonnegative weighting function that is larger in regions that are more sensitive to variability. The second cost function is inversely proportional to the variability:

$$f_2 = \int_0^1 \frac{1}{\sigma(s)}\, ds. \tag{6.3}$$

We determine the standard deviation field $\sigma^*(s)$ that minimizes the sum of the two cost functions:

$$\sigma^*(s) = \arg\min_{\sigma(s)}, \quad f := f_1 + f_2. \tag{6.4}$$

This model problem is analogous to a tolerance optimization problem, where the improvements in the mean performance are balanced by the costs of reducing tolerances.

Reducing tolerances (decreasing the variance $\sigma^2(s)$) improves the mean performance of the system, which is reflected in the cost function f_1. Introducing variability into certain regions of the domain has a larger impact on the mean performance, as expressed by the weight function $w(s)$. It is also costly to reduce tolerances, and the cost of reducing tolerances increases monotonically, as reflected in the form of f_2.

The optimal solution to (6.4) can be derived analytically using the calculus of variations. The expectation and spatial integration can be interchanged in (6.2) to give

$$f_1 = \int_0^1 \mathbb{E}[e^2(x,\theta)]w(x)\ dx = \int_0^1 \sigma^2(x)w(x)\ dx. \tag{6.5}$$

The first variation of f can then be computed directly:

$$\delta f = \int_0^1 \left(2\sigma(x)w(x) - \frac{1}{\sigma^2(x)}\right)\delta\sigma(x)\ dx. \tag{6.6}$$

Enforcing stationarity by setting $\delta f = 0$, the optimal standard deviation field is found to be

$$\sigma^*(x) = \left[\frac{1}{2w(x)}\right]^{1/3}. \tag{6.7}$$

This optimum is unique since both f_1 and f_2 are strictly convex functionals.

As an example, we choose the weight function to be $w(x) = 2 + \sin(2\pi x)$. The standard deviation field is discretized with $N_\sigma = 20$ cubic B-spline basis functions B_i:

$$\sigma(x) = \sum_{i=1}^{N_\sigma} \sigma_i B_i(x). \tag{6.8}$$

The mean performance of engineering systems typically cannot be computed in closed form, and instead must be estimated. We therefore use the Monte Carlo method to compute an unbiased estimate of f_1, rather than computing it directly from (6.5):

$$\hat{f}_1 = \frac{1}{N}\sum_{n=1}^{N}\int_0^1 e_n^2(s)w(s)\ ds. \tag{6.9}$$

For each Monte Carlo sample, the integral is evaluated using composite Gaussian quadrature with 20 intervals and a third-order rule on each interval. The same quadrature rule is used to estimate f_2. The SAA equivalent of (6.4) results from replacing the objective function f_1 with its unbiased estimate:

$$\hat{\sigma}^*(s) = \underset{\sigma(s)}{\arg\min}, \quad \hat{f}_1 + f_2. \tag{6.10}$$

This optimization problem is solved using the SQP method with a BFGS update to approximate the Hessian as implemented in the NLopt package [20]. The pathwise estimate of the sensitivity $\partial f_1/\partial\sigma(s)$, which is an unbiased estimate of the true gradient, is computed as

$$\frac{\partial \hat{f}_1}{\partial \sigma} = \frac{1}{N}\sum_{n=1}^{N}\int_0^1 2w(s)e_n(s)\frac{\partial e_n}{\partial \sigma}\ ds. \tag{6.11}$$

The sample path sensitivity $\partial e_n/\partial\sigma$ can be computed using either approach described previously, i.e., by computing the sensitivity of the K-L expansion or by computing sensitivities for a unit-variance random field scaled by $\sigma(x)$. We use both approaches to compare their effectiveness. The optimizations are initialized by setting $\sigma(x) = 0.6$ everywhere, and were terminated when the relative change in the objective function was less than 1.0×10^{-9}. To construct the K-L expansion, the integral in (2.4) is approximated using the same composite Gaussian quadrature used to approximate the objective functions f_1 and f_2, and the resulting eigenproblem is solved to determine the λ_i and ϕ_i in the K-L expansion (2.6). All realizations of the random field were simulated using $N_{KL} = 11$ K-L modes, which ensured that the partial scatter exceeded 99.9%.

Figures 3 and 4 compare sample optimal solutions obtained using each method of computing sensitivities with the true solution. The 95% confidence region is computed by estimating the Hessian matrix $\mathbf{B}$ and covariance $\mathbf{\Sigma}$ using the Monte Carlo samples used to compute the optimal solution:

$$\hat{\mathbf{B}} = \frac{1}{N}\sum_{n=1}^{N} \nabla^2 J(\hat{\sigma}^*), \tag{6.12}$$

$$\hat{\mathbf{\Sigma}} = \frac{1}{N}\sum_{n=1}^{N} \nabla J(\hat{\sigma}^*)\nabla J(\hat{\sigma}^*)^\intercal, \tag{6.13}$$

where

$$J = \int_0^1 \frac{1}{\sigma(s)} + e^2(s,\theta)w(s)\ ds. \tag{6.14}$$

The standard error of the optimal solution is then $\varepsilon_N = [\mathrm{diag}(\hat{\mathbf{B}}^{-1}\hat{\mathbf{\Sigma}}\hat{\mathbf{B}}^{-1})/N]^{1/2}$ [28]. The plots show that the true optimal solution is largely within the 95% confidence region for each approximate solution. Qualitatively, for a given number of Monte Carlo samples, the solutions obtained using either sensitivity approach are very similar.

To further illustrate the convergence of the SAA optimal solution to the true optimal solution, we conduct $M = 10^4$ independent optimization runs for different values of N. This allows us to examine the distribution of the approximate optimal solution. Since the computational cost of using a scaled unit-variance random field is lower, we use this method to perform each optimization. Figure 5 shows histograms of the error of the SAA optimal solution evaluated at the center of the domain, i.e., $\hat{\sigma}^*_N(0.5) - \sigma^*(0.5)$, for various values of N. As expected, the histograms closely resemble Gaussian distributions with standard deviation proportional to $N^{-1/2}$. Figure 6 illustrates the convergence of the entire optimal solution and optimal value as N is increased. The standard deviation of the optimal solution error $\hat{\sigma}^*_N(x) - \sigma^*(x)$ is plotted on the left, and the standard deviation of the optimal value error $f(\hat{\mathbf{p}}^*_N) - f(\mathbf{p}^*)$ is plotted on the right. Both converge like $N^{1/2}$: increasing the number of Monte Carlo samples by a factor of 100 gains a one decimal improvement in solution accuracy. Table 1 compares the average number objective and gradient evaluations required for the different numbers of Monte Carlo samples, illustrating that increasing the number of Monte Carlo samples does not have a significant impact on the convergence of the optimization.

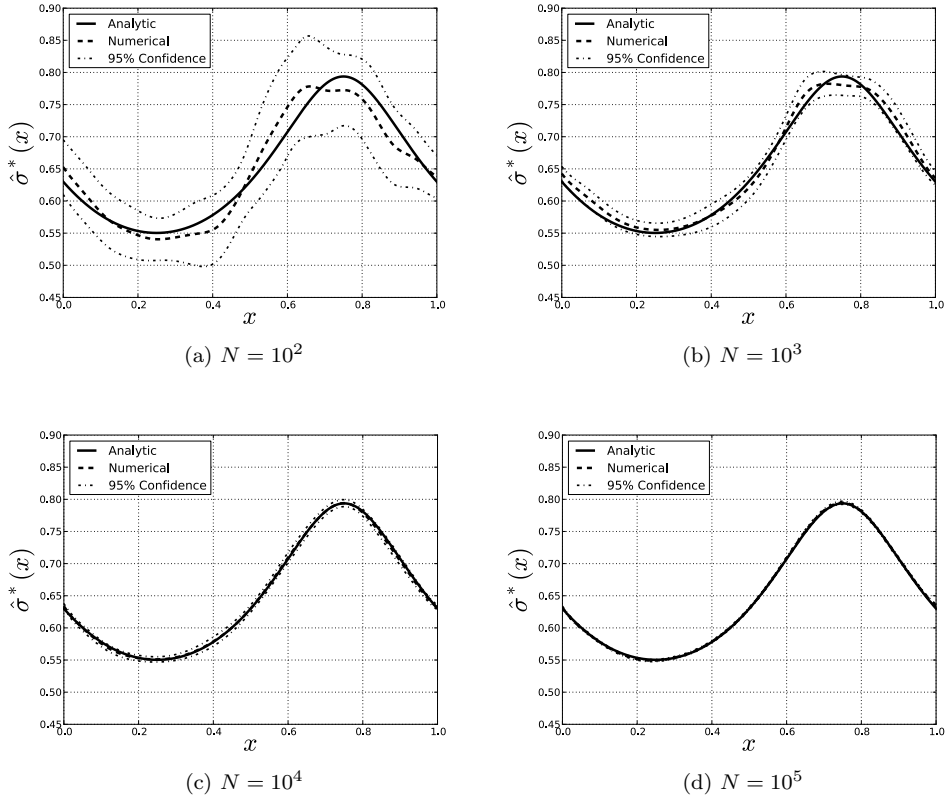

(a) $N = 10^2$ (b) $N = 10^3$

(c) $N = 10^4$ (d) $N = 10^5$

FIG. 3. *Optimal solutions obtained with an increasing number of Monte Carlo samples. The gradient information used to obtain $\hat{\sigma}^*$ is computed using the sensitivity of the K-L expansion.*

7. Application: compressor blade tolerance optimization. We now apply the proposed optimization framework to a problem with engineering relevance: manufacturing tolerance optimization. Specifically, we consider a gas turbine compressor blade geometry that is subject to random manufacturing errors. We optimize the manufacturing tolerances to provide the greatest performance benefit.

7.1. Manufacturing error and tolerance models. Previous studies of geometric variability in compressor blades have indicated that the discrepancy between manufactured blade geometries and the design intent geometry can be accurately modeled as a Gaussian random field [2, 11, 14, 31]. In this context, the random field $e(x, \theta)$ represents the error between the manufactured surface and the nominal surface in the normal direction at the point x on the nominal blade surface. The mean of the manufacturing error is assumed to be zero everywhere, i.e., $\bar{e}(x) = 0$.

Manufacturing variability tends to negatively impact the mean performance of compressor blades. We quantify the performance of a compressor blade in terms of the total pressure loss coefficient, denoted by $\bar{\omega}$. Higher losses reduce the efficiency of the compressor, which corresponds to higher fuel burn. Previous investigations of the impact of manufacturing variability have shown that the mean loss of compressor blades tends to increase as the level of variability, i.e., the variance of the random field $e(x, \theta)$, is increased [14, 18]. It is possible to reduce this detrimental impact by

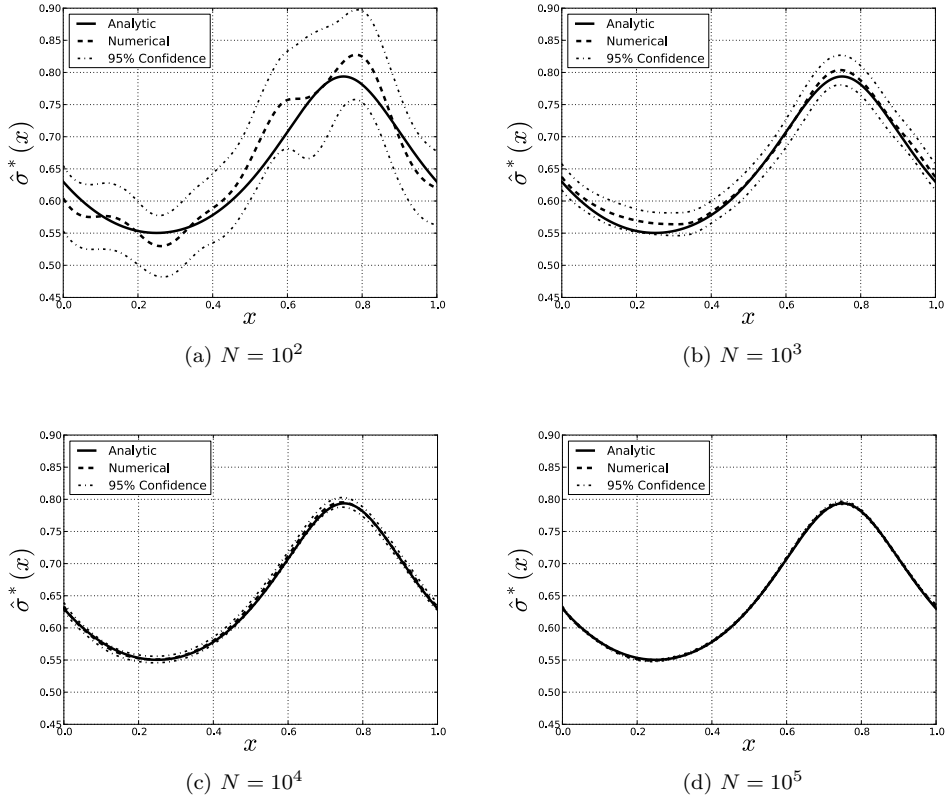

(a) $N = 10^2$ (b) $N = 10^3$

(c) $N = 10^4$ (d) $N = 10^5$

FIG. 4. *Optimal solutions obtained with increasing number of Monte Carlo samples. The gradient information used to obtain $\hat{\sigma}^*$ is computed using a scaled unit-variance random field.*

specifying tighter manufacturing tolerances, thereby reducing the standard deviation $\sigma(x)$ of the surface variations. However, specifying stricter tolerances incurs higher manufacturing costs. The objective of improving the mean performance therefore competes with the objective of reducing manufacturing costs.

It is known that reducing the manufacturing variability in some regions of the blades has a higher impact on the mean performance than in others. For example, Garzon found that geometric variations near the leading edge are primarily responsible for increasing mean loss of a transonic compressor blade [14]. The proposed tolerance optimization approach therefore reduces $\sigma(x)$ only in the regions with the largest impact on the mean performance, ensuring the manufacturing costs remain low. To do this, we first define the variability metric V, which measures the total level of manufacturing variations over the entire blade surface:

$$V(\boldsymbol{\sigma}) = \int_X \sigma(x)\, dx. \tag{7.1}$$

Here $\boldsymbol{\sigma} \in \mathbb{R}^{N_\sigma}$ parameterizes the standard deviation $\sigma(x)$. To constrain the manufacturing cost, we constrain the variability metric to a specified value V_b, representing the strictest tolerances deemed acceptable by the manufacturer. The standard deviation of the manufacturing variability is constrained from above to ensure the optimizer

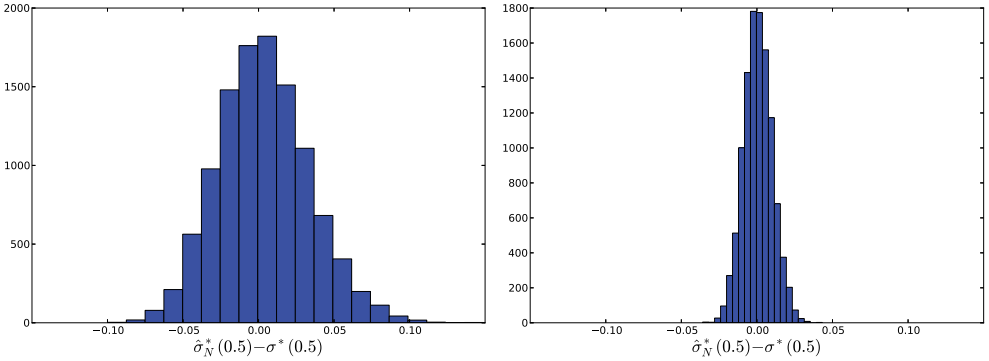

(a) $N = 10^2$ (b) $N = 10^3$

(c) $N = 10^4$ (d) $N = 10^5$

FIG. 5. *Histograms of the error at the center of the domain* $\hat{\sigma}_N^*(0.5) - \sigma^*(0.5)$ *for an increasing number of Monte Carlo samples.*

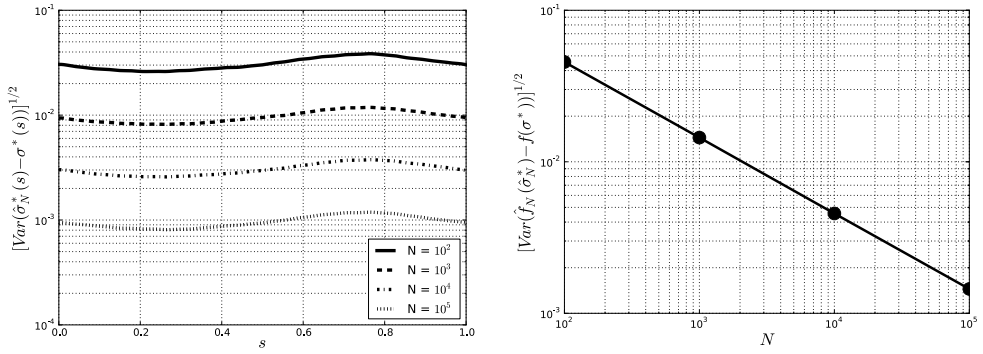

(a) (b)

FIG. 6. *Standard deviations of the optimal solution* (a) *and optimal solution value* (b).

does not trade increases in variability in regions of low sensitivity for excessive decreases in variability in regions of high sensitivity, thereby driving $\sigma(x)$ to zero in some of the regions of low sensitivity.

Turbomachinery designers are typically interested in the performance over a range of operating conditions, e.g., over a range of flow incidence angles. We therefore

minimize the weighted mean loss over a set of incidence angles $\{\alpha_i\}_{i=1}^{N_p}$ and introduce the weight vector $\mathbf{w} \in \mathbb{R}^{N_p}$ that weighs the relative importance of the mean loss at different incidence. The optimization problem for the optimal tolerances is given below:

$$\begin{aligned} \boldsymbol{\sigma}^* = \quad & \arg\min_{\boldsymbol{\sigma}} \quad \sum_{i=1}^{N_p} w_i \mathbb{E}[\bar{\omega}(\boldsymbol{\sigma}; \alpha_i)] \\ & \text{s.t.} \quad V(\boldsymbol{\sigma}) = V_b, \\ & \qquad \sigma(x) \leq \sigma_{max}. \end{aligned} \tag{7.2}$$

To solve (7.2) numerically, the SAA method is used and all objective and constraint functions are replaced by their Monte Carlo estimates. The resulting nonlinear optimization problem is solved using SQP. The gradient of the objective and constraints is computed using the pathwise approach described previously, and the shape sensitivities are evaluated using second-order accurate finite differences.

TABLE 1
Average number of objective and gradient evaluations required for different numbers of Monte Carlo samples.

N	# of objective evaluations	# of gradient evaluations
10^2	29.4	29.4
10^3	26.8	26.8
10^4	26.7	26.7
10^5	26.9	26.9

7.2. Flow solver. All flow solutions are computed using the MISES (Multiple blade Interacting Streamtube Euler Solver) [10] turbomachinery analysis code. The boundary layer and wake regions are modeled using an integral boundary layer equation formulation describing the evolution of the integral momentum and kinetic energy shape parameter. In the inviscid regions of the flow field, the steady state Euler equations are discretized over a streamline conforming grid. Transition models are included to predict the onset of turbulent flow in the boundary layer.

A convenient feature of MISES is its solution speed. A typical flow solution requires 10–20 Newton-Raphson iterations to converge, which can be performed in a few seconds. Moreover, MISES offers the option to reconverge a flow solution after perturbing the airfoil geometry. Since the perturbations in the geometry introduced by manufacturing variability are small, the flow field corresponding to blades with manufacturing variability can be reconverged very quickly from the flow field computed for the nominal geometry. This offsets some of the computational cost associated with using the standard Monte Carlo method to propagate uncertainty.

7.3. Numerical results. We apply the proposed method to optimize the tolerances of a two-dimensional compressor rotor blade. The geometry is chosen to be Standard Configuration 10 (SC10) rotor blade, which is a modified NACA0006 airfoil with a circular camber line [13]. For this case, the inlet Mach number is $M_1 = 0.7$ and the inflow angle is $\beta_1 = 53.5°$. Following [26], a Reynolds number based on the blade chord of 1.26×10^6 is used, and the inlet turbulence intensity is set to 4%.

Manufacturing variations are prescribed in the form of a Gaussian random field with standard deviation 6.0×10^{-4} (nondimensionalized by the blade chord). The covariance function of the random field is the same squared exponential function described earlier, with a correlation length that is reduced near the leading edge of the blade to reflect the small correlation length features observed in the leading edges of measured blades [14, 21]. Specifically, the correlation length is given by $L = \sqrt{L'(s_1)L'(s_2)}$, where

$$L'(s) = L_0 + (L_{LE} - L_0)\exp[-(s/w)^2]. \tag{7.3}$$

At the leading edge, the correlation length (nondimensionalized by the blade chord) is $L_{LE} = 0.0095$, and the correlation length smoothly increases to $L_0 = 0.4$ away from the leading edge. The parameter w describes the extent of the leading edge and is chosen to be equal to the radius of curvature of the leading edge, which was 3.8% of the blade chord.

To represent the standard deviation field $\sigma(x)$ over the surface of the blade, we use the same cubic B-spline basis introduced previously. The knot placement is chosen to enrich the basis near the leading edge, since previous studies of the impact of geometric variability on compressor performance have shown that most of the increase in loss results from imperfections near the leading edge. The knot spacing of $\Delta x = 3.0 \times 10^{-3}$ at the leading edge. The knot spacing grows towards the trailing edge on either side of the blade until 10% of the chord, after which it is held fixed. The resulting basis represents $\sigma(x)$ using $N_\sigma = 41$ basis functions. To compute the K-L expansion, fourth-order composite Gaussian quadrature was used to approximate the integral in (2.4) with 100 equally spaced intervals. $N_{KL} = 16$ K-L modes were used to simulate the random field, which ensured that the partial scatter exceeded 99.9%.

The total allowable variability V_b was constrained to be 98% of the baseline level of variability, and the standard deviation was constrained to be below $\sigma_{max} = 6.0 \times 10^{-4}$ everywhere on the blade surface. We use $N_p = 3$ design points at $\alpha = -5°$, $0°$, and $5°$ with the weight vector $\mathbf{w} = \{1/4,\ 1/2,\ 1/4\}$. The optimization was terminated when the objective function converged within an absolute tolerance of 10^{-5}, and a total of 31 SQP iterations were required to obtain the optimal solution. Each SQP iteration requires evaluating one evaluation of the gradient of the objective and constraint functions, as well as a number of evaluations of the objective and constraint functions to perform a linesearch. The objectives and constraints were evaluated using $N = 500$ Monte Carlo samples. For each Monte Carlo sample, the gradient of the objectives and constraints with respect to the B-spline coefficients that parameterize $\sigma(x)$ are computed using finite differences. The optimization is initialized by setting $\sigma(x) = 6.0 \times 10^{-4}$ everywhere on the blade surface.

The optimized tolerances are shown in Figure 7. We only show the standard deviation near the leading edge of the blade, since the optimal value over the rest of the blade was equal to the baseline value of 6.0×10^{-4}. The performance impact of optimizing the tolerances is illustrated in Figure 8, which shows the loss coefficient of the nominal blade as well as the mean loss coefficient for the blade with uniform tolerances ($\sigma(x) = 6.0 \times 10^{-4}$) and optimized tolerances for a range of incidence angles. With uniform tolerances, manufacturing variability increases the mean loss by an average of 6% over the range of incidence angles considered. The increase in the mean loss coefficient at both positive and negative incidence is a result of flow

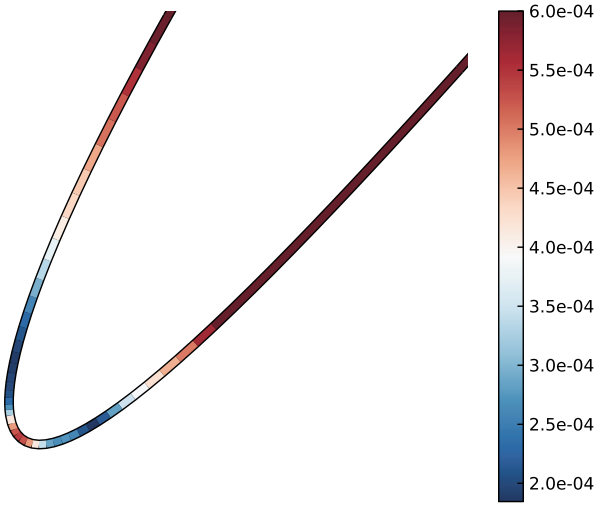

FIG. 7. *Optimal distribution of the standard deviation $\sigma(x)$ near the leading edge.*

separation, where the flow reverses direction near the blade surface, increasing the mixing losses. Restricting the tolerances on the lower surface reduces the extent of separation at negative incidence and restricting the tolerances on the upper surface reduces the extent of separation at positive incidence. The optimized tolerances reduce the shift in loss by an average of 78% over the range of incidences shown in Figure 8. Thus, for a small decrease in the level of manufacturing variability, a significant decrease in the mean loss is achieved, demonstrating the efficacy of the proposed approach.

8. Summary and conclusions. This paper has presented an approach for optimizing the mean and covariance of Gaussian random fields to achieve a desired statistical performance. Sample path sensitivities with respect to the covariance function were derived from the Karhunen–Loève expansion. This sensitivity analysis allows for gradient-based algorithms to be leveraged when optimizing random fields. We applied gradient-based optimization to design the manufacturing tolerances of a compressor blade by reducing variability in the regions of the blade where geometric variability has the largest impact on the mean performance.

Future work should incorporate the adjoint method of computing sensitivities when considering PDE-constrained problems. The adjoint method can be used to compute the functional derivative $\partial F_n/\partial e_n$ when the quantity of interest F is computed from the solution of a PDE by solving a set of adjoint equations derived from the linearized PDE [19]. The computational cost of computing sensitivities with the adjoint method grows with the number of objectives and constraints, but is independent of the number of design variables. Thus, the adjoint method is well suited to engineering design applications where the number of design variables is typically large relative to the number of objectives and constraints.

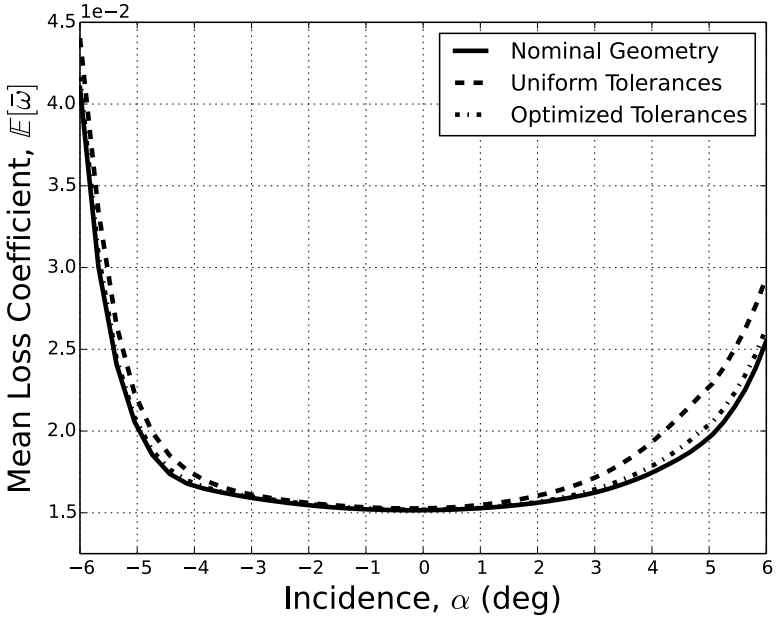

FIG. 8. *Mean loss for the nominal geometry, manufactured blades with uniform tolerances, and manufactured blades with optimized tolerances.*

REFERENCES

[1] P. ABRAHAMSEN, *A Review of Gaussian Random Fields and Correlation Functions*, Technical Report TR-917, Norwegian Computing Center, Oslo, Norway, 1997.

[2] B. B. BEACHKOFSKI AND R. V. GRANDHI, *Probabilistic system reliability for a turbine engine airfoil*, in Proceedings of ASME Turbo Expo 2004, pp. 171–179.

[3] H. G. BEYER AND B. SENDHOFF, *Robust optimization–A comprehensive survey*, Comput. Methods Appl. Mech. Engrg., 196 (2007), pp. 3190–3218.

[4] P. T. BOGGS AND J. W. TOLLE, *Sequential quadratic programming*, in Acta Numerica, Cambridge University Press, Cambridge, UK, 1995, pp. 1–51.

[5] A. BORZÌ, V. SCHULZ, C. SCHILLINGS, AND G. VON WINCKEL, *On the treatment of distributed uncertainties in PDE-constrained optimization*, GAMM-Mitt., 33 (2010), pp. 230–246.

[6] M. BROADIE AND P. GLASSERMAN, *Estimating security price derivatives using simulation*, Management Science, 42 (1996), pp. 269–285.

[7] S. CHEN, W. CHEN, AND S. LEE, *Level set based robust shape and topology optimization under random field uncertainties*, Struct. Multidiscip. Optim., 41 (2010), pp. 507–524.

[8] G. CHRISTAKOS, *Random Field Models in Earth Sciences*, Dover, New York, 2012.

[9] J. DE LEEUW, *Derivatives of Generalized Eigen Systems with Applications*, Technical Report TR-528, UCLA, Department of Statistics, Los Angeles, CA, 2007.

[10] M. DRELA AND M. B. GILES, *Viscous-inviscid analysis of transonic and low Reynolds number airfoils*, AIAA J., 25 (1986), pp. 1347–1355.

[11] J. D. DUFFNER, *The Effects of Manufacturing Variability on Turbine Vane Performance*, Master's dissertation, Massachusetts Institute of Technology, Department of Aeronautics and Astronautics, Cambridge, MA, 2008.

[12] G. PAPANICOLAOU, J. P. FOUQUE, K. SOLNA, AND R. SIRCAR, *Singular perturbations in option pricing*, SIAM J. Appl. Math., 63 (2003), pp. 1648–1665.

[13] T. H. FRANSSON AND J. M. VERDON, *Standard configurations for unsteady flow through vibrating axial-flow turbomachine cascades*, in Unsteady Aerodynamics, Aeroacoustics and Aeroelasticity of Turbomachines and Propellers, H. M. Atassi, ed., Springer-Verlag, New

York, 1993, pp. 859–889.
[14] V. E. Garzon, *Probabilistic Aerothermal Design of Compressor Airfoils*, Ph.D. dissertation, Massachusetts Institute of Technology, Department of Aeronautics and Astronautics, Cambridge, MA, 2003.
[15] T. Gerstner and M. Griebel, *Numerical integration using sparse grids*, Numer. Algorithms, 18 (1998), pp. 209–232.
[16] M. B. Giles and N. A. Pierce, *An introduction to the adjoint approach to design*, Flow, Turbulence and Combustion, 65 (2000), pp. 393–415.
[17] P. Glasserman, *Monte Carlo Methods in Financial Engineering*, Appl. Math. (N.Y.) 53, Springer-Verlag, New York, 2004.
[18] M. N. Goodhand, R. J. Miller, and H. W. Lung, *The sensitivity of 2D compressor incidence range of in-service geometric variation*, in Proceedings of the ASME Turbo Expo 2012, 2012, pp. 159–170.
[19] A. Jameson, *Aerodynamic design via control theory*, in Recent Advances in Computational Fluid Dynamics, Lecture Notes in Engrg., 43, Springer, Berlin, 1989, pp. 377–401.
[20] S. G. Johnson, *The NLopt nonlinear-optimization package*, available online at http://ab-initio.mit.edu/nlopt, 2013.
[21] A. Lange, M. Voigt, K. Vogeler, and E. Johann, *Principal component analysis on 3D scanned compressor blades for probabilistic CFD simulation*, in Proceedings of the 53rd AIAA/ASME/ASCE/AHS/ASC Structures, Structural Dynamics and Materials Conference, 2012.
[22] O. P. Le Mâitre and O. M. Knio, *Spectral Methods for Uncertainty Quantification–With Applications to Computational Fluid Dynamics*, Springer, New York, 2010.
[23] J. R. Magnus and H. Neudecker, *Matrix Differential Calculus with Applications in Statistics and Econometrics*, 3rd ed., John Wiley & Sons, New York, 2007.
[24] J. Nocedal and S. J. Wright, *Numerical Optimization*, 2nd ed., Springer, New York, 2006.
[25] E. J. Nyström, *On the practical solution of integral equations with applications to boundary value problems*, Acta Math., 54 (1930), pp. 185–204.
[26] P. J. Petrie-Repar, A. McGhee, and P. A. Jacobs, *Three-dimensional viscous flutter analysis of standard configuration* 10, in Proceedings of the ASME Turbo Expo 2007, 2007, pp. 665–674.
[27] M. M. Putko, A. C. Tyalor, P. A. Newman, and L. L. Green, *Approach for input uncertainty propagation and robust design in CFD using sensitivity derivatives*, J. Fluids Engineering, 124 (2002), pp. 60–69.
[28] R. Y. Rubinstein and A. Shapiro, *Discrete Event Systems: Sensitivity Analysis and Stochastic Optimization by the Score Function Method*, John Wiley & Sons, Ltd., Chichester, UK, 1993.
[29] C. Schillings, S. Schmidt, and V. Schulz, *Efficient shape optimization for certain and uncertain aerodynamic design*, Comput. & Fluids, 46 (2011), pp. 78–87.
[30] P. W. Sheppard, M. Rathinam, and M. Khammash, *A pathwise derivative approach to the computation of parameter sensitivities in discrete stochastic chemical systems*, J. Chem. Phys., 136 (2012), 034115.
[31] A. Sinha, B. Hall, B. Cassenti, and G. Hilbert, *Vibratory parameters of blades from coordinate measurement machine data*, J. Turbomach., 130 (2008), 011013.